THE JOURNAL OF BIOLOGICAL CHEMISTRY VOL. 290, NO. 26, pp. 16132–16141, June 26, 2015

A Novel Mutation in Isoform 3 of the Plasma Membrane Ca^{2+} Pump Impairs Cellular Ca^{2+} Homeostasis in a Patient with Cerebellar Ataxia and Laminin Subunit 1α Mutations*

Received for publication, April 2, 2015, and in revised form, May 6, 2015 Published, JBC Papers in Press, May 7, 2015, DOI 10.1074/jbc.M115.656496

Tito Calì[‡1,2], Raffaele Lopreiato[§2], Joshua Shimony[¶], Marisa Vineyard[‖], Martina Frizzarin[§], Ginevra Zanni[**], Giuseppe Zanotti[§], Marisa Brini[‡3], Marwan Shinawi[‖4], and Ernesto Carafoli[‡‡5]

*From the Departments of [‡]Biology and [§]Biomedical Sciences University of Padova, 35131 Padova, Italy, [¶]Mallinckrodt Institute of Radiology and [‖]Department of Pediatrics, Division of Genetics and Genomic Medicine, Washington University School of Medicine, St. Louis, Missouri 63110-1093, **Unit of Molecular Medicine for Neuromuscular and Neurodegenerative Disorders, Department of Neurosciences, Bambino Gesù Children's Hospital, Istituti di Ricovero e Cura a Carattere Scientifico (IRCCS), 00165 Rome, Italy, and [‡‡]Venetian Institute of Molecular Medicine (VIMM), 35131 Padova, Italy*

Background: Mutations in plasma membrane Ca^{2+}-ATPase (PMCA) isoform 3 and in laminin subunit 1α have previously been linked to ataxic phenotypes.
Results: A novel PMCA3 missense mutation co-occurring with a compound heterozygous mutation in laminin subunit 1α impaired cellular Ca^{2+} homeostasis.
Conclusion: The two mutations could work synergistically to generate the disease phenotype.
Significance: A digenic mechanism could be responsible for this case of cerebellar ataxia.

The particular importance of Ca^{2+} signaling to neurons demands its precise regulation within their cytoplasm. Isoform 3 of the plasma membrane Ca^{2+} ATPase (the PMCA3 pump), which is highly expressed in brain and cerebellum, plays an important role in the regulation of neuronal Ca^{2+}. A genetic defect of the PMCA3 pump has been described in one family with X-linked congenital cerebellar ataxia. Here we describe a novel mutation in the *ATP2B3* gene in a patient with global developmental delay, generalized hypotonia and cerebellar ataxia. The mutation (a R482H replacement) impairs the Ca^{2+} ejection function of the pump. It reduces the ability of the pump expressed in model cells to control Ca^{2+} transients generated by cell stimulation and impairs its Ca^{2+} extrusion function under conditions of low resting cytosolic Ca^{2+} as well. *In silico* analysis of the structural effect of the mutation suggests a reduced stabilization of the portion of the pump surrounding the mutated residue in the Ca^{2+}-bound state. The patient also carries two missense mutations in *LAMA1*, encoding laminin subunit 1α. On the basis of the family pedigree of the patient, the presence of both PMCA3 and laminin subunit 1α mutations appears to be necessary for the development of the disease. Considering the observed defect in cellular Ca^{2+} homeostasis and the previous finding that PMCAs act as digenic modulators in Ca^{2+}-linked pathologies, the PMCA3 dysfunction along with *LAMA1* mutations could act synergistically to cause the neurological phenotype.

Ca^{2+} regulates most of the activities of eukaryotic cells, therefore, it must be very precisely regulated in the cell ambient in both time and space (1, 2). A number of mechanisms contribute to the regulation of cell Ca^{2+}, from soluble proteins that reversibly bind it, to protein systems that mediate its transport across membranes. A distinctive property of Ca^{2+} as a carrier of cellular signals is ambivalence: if its precise regulation fails, Ca^{2+} becomes a messenger of cell discomfort or even death (2). Unfortunately, failures of regulation occur in numerous disease cases, causing various degrees of cellular dysfunction. Ca^{2+}-ATPases (Ca^{2+} pumps) are of special importance in the process of Ca^{2+} control: their malfunctioning is a frequent causative agent in important disease states.

Since neurons are particularly dependent on the perfect regulation of their own Ca^{2+} (3), a number of neuronal diseases reflect the incorrect functioning of the Ca^{2+} controlling systems. Among these disease states, those linked to defects of the plasma membrane Ca^{2+} ATPase (PMCA)[6] pumps are becoming increasingly important. In mammals, PMCA pumps are the products of 4 genes. The 4 basic isoforms are organized in the plasma membrane with 10 transmembrane domains and a long cytosolic C-terminal tail that contains the regulatory domains of the enzyme (4). 2 of the 4 basic isoforms (PMCA2 and -3) have tissue-restricted distribution, and are particularly abundant in the brain and the cerebellum. They have high affinity for calmodulin, which interacts with the cytosolic C-terminal tail

* This work was supported by the University of Padova (local grants (to-M. B.), Progetto Giovani GRIC128SP0 (to T. C.), and Progetto di Ateneo CPDA115047/11 (to R. L.)).
[1] Supported by the University of Padova (Progetto Giovani GRIC128SP0, Bando 2012).
[2] Both authors contributed equally to this work.
[3] To whom correspondence may be addressed: Dept. of Biology, University of Padova, 35131 Padova, Italy. E-mail: marisa.brini@unipd.it.
[4] To whom correspondence may be addressed: Dept. of Pediatrics, Division of Genetics and Genomic Medicine, Washington University in St Louis, St Louis, MO 63110-1093. E-mail: Shinawi_M@kids.wustl.edu.
[5] To whom correspondence may be addressed: Venetian Institute of Molecular Medicine (VIMM), 35131 Padova, Italy. E-mail: ernesto.carafoli@unipd.it.

[6] The abbreviations used are: PMCA, plasma membrane Ca^{2+} ATPase; ER, endoplasmic reticulum; SOCE, store-operated Ca^{2+} entry; $InsP_3$, inositol 1,4,5 trisphosphate.

of the pumps, removing it from binding sites next to the active center of the pumps, relieving the state of auto-inhibition (4).

PMCA2 and PMCA3 concentrate in the cerebellum with complementary distribution: PMCA3 is mostly associated with the axonal terminal of granule neurons, while PMCA2 is particularly abundant in Purkinje dendrites. PMCA3 is also prominently expressed in the choroid plexus (5), and a particular splice variant of PMCA2 is located in the stereocilia of the outer hair cells of the inner ear (6). Genetic defects of the PMCA pumps have been described for PMCA2 and PMCA3. A series of mutations of the former in mice and humans cause deafness (7–9). Interestingly, the deafness phenotype was not the only associated phenotype: one of the PMCA2-defective mice also had prominent ataxic symptoms (10). The PMCA2 knock-out mice exhibited ataxic phenotype, with cerebellar dysfunctions associated with shrunken Purkinje neurons dendrites and reduced firing frequency (11). As for PMCA3, a missense mutation of a residue in the C-terminal calmodulin-binding domain has been recently identified and studied in a family with X-linked congenital cerebellar ataxia associated with cerebellar atrophy (12). This mutation reduced the ability of the PMCA3 pump to restore the concentration of Ca^{2+} to baseline after the transient increase induced by stimulation with an inositol 1,4,5 trisphosphate ($InsP_3$) generating agonist, which induced Ca^{2+} release from intracellular stores.

In the present study we describe a patient with global developmental delay, generalized hypotonia and cerebellar ataxia associated with a novel missense mutation in the gene encoding the PMCA3 pump. We have analyzed possible Ca^{2+} handling defects associated with the mutation by expressing the mutant pump in model cells and have found that both the Ca^{2+} extrusion under resting cell conditions, and the control of cytosolic Ca^{2+} transients generated upon cell stimulation were compromised. The proband also carried two missense mutations in the *LAMA1* gene coding for laminin subunit 1α. This is an interesting finding as it recalls the digenic mechanism described in the case of hereditary human deafness, where the mutations of the PMCA2 pump were accompanied by mutations of cadherin-23, a protein involved in the mechanoelectrical transduction process (7, 9).

The presence of two *LAMA1* genetic mutations in our proband is of particular interest, as a phenotype of cerebellar dysplasia with cysts (with and without retinal dystrophy) has recently been described in 7 probands who carried homozygous or compound heterozygous mutations, or deletion mutations in the *LAMA1* gene which induce protein truncation (13). Our patient displays clinical features of X-linked cerebellar ataxia. His brain imaging showed unusual vertical course of the straight sinus with inferior location of the torcula consistent with a relatively small posterior fossa. Since the same PMCA3 mutation was found in the healthy maternal grandfather, the PMCA3 pump defect is evidently not sufficient to cause the neurological phenotype *per se*. On the other hand, since no individual harboring exclusively the two *LAMA1* mutations has been identified so far, it is not possible to state conclusively that the phenotype in our proband could be entirely associated with the double *LAMA1* defect. Considering the increasing number of reports implicating PMCA pump defects in neuronal diseases and, especially, the previous finding of the digenic origin of the phenotype in patients carrying PMCA2 mutations (7), it is plausible to suggest that the PMCA3 mutation could act as an essential digenic modulator in the development of cerebellar dysgenesis associated to *LAMA1* mutations.

Experimental Procedures

Molecular Analysis—Exome sequencing was performed by GeneDx (Gaithersburg, MD) using Agilent SureSelect XT2 All Exon V4 Kit and Illumina HiSeq 2000 with 100bp paired-end reads. Sequence was aligned to the UCSC build hg19 reference sequence. Mean depth of coverage was 121x with quality threshold of 98.9%. GeneDx's XomeAnalyzer was used to evaluate sequence changes found between the proband, parental samples, and reference. Di-deoxy sequencing was used for confirmation of reported mutations.

DNA Constructs—Full-length (PMCA3*b*) and truncated (*PMCA3a*) variants of PMCA3 R482H mutant were obtained by site-directed mutagenesis on cDNA templates of human origin cloned in the pcDNA3 vector. Mutagenesis was performed according to the manufacturer's standard protocol (Stratagene, Cedar Creek, TX) using the following primers R482H-for 5′-GGCACGCTCACCACCAAC**CAT**ATGACCGTGGTCCAGTCC-3′; R482H-rev 5′- GGACTGGACCACGGTCAT**AT-G**GTTGGTGGTGAGCGTGCC-3′. To create yeast expression vectors wild-type human PMCA3b cDNA was amplified by PCR using high-fidelity DNA polymerase (KAPA Biosystems) and the following primers: PMCA3b-for: 5′-GCTTGGTACCGAGCTCGGATCCGTCGACATGGGTGACATGGCGAACAGTTCC-3′; PMCA3b-rev: 5′-CATGCT CGAGCGGCCGCTTAGAGGGATGTCTCCATGCTGTGG-3′. The wild-type PMCA3b-pYES2 vector was used a template to generate the R482H PMCA3b-pYES2 vectors and the other two control mutants. The constitutively inactive PMCA3 D459A mutant was created by PCR using the following primers: D459A-for: 5′-ACAGCCATCTGTTCT**GCC**AAGACAGGCACACTC-3′, and D459A-rev 5′-GAGTGTGCCTGTCTT **GGC**AGAACAGATGGCTGT-3′. The constitutively active PMCA3-ΔCter was created by deleting the last 158 residues at its C terminus by PCR amplification of the wt PMCA3b cDNA template using the PMCA3b-for and the PMCA3ΔC-rev: 5′-CATGCTCGAGCGGCCGCTTACTGGCTGGTGGGGATAGTGGC-3′ primers. The PCR products were digested by KpnI and XhoI restriction enzymes and inserted in the galactose-inducible pYES2 plasmid (Life Technologies). The mutated codons are in bold and the restriction sites are underlined. All the constructs were verified by sequencing. cytAEQ expression plasmid has been previously described (14).

Cell Cultures and Transfection—HeLa cells were obtained from ATCC Cell Biology Collection. They were grown in Dulbecco's modified Eagle's medium high glucose (DMEM, Euroclone), supplemented with 10% fetal bovine serum (FBS, Euroclone), 100 units/ml penicillin and 100 μg/ml streptomycin; 12 h before transfection, cells were seeded onto 6-multiwell plates (for aequorin measurements and Western blotting analysis) or 13-mm glass coverslips (for immunocytochemistry analysis) and allowed to grow to 60 – 80% confluence. For Ca^{2+} measurements HeLa cells were co-transfected with the

aequorin construct (cytAEQ) and the empty vector (mock) or PMCA3 expressing plasmids in a 1:2 ratio with the calcium-phosphate procedure as previously described (15). 6 μg of total plasmid DNA were used for the transfection of the cells in each well of the 6-multiwell plate and 4 μg for each 13-mm coverslip.

Western Blotting Analysis—48 h after transfection Hela cells were washed on ice with Ca^{2+}/Mg^{2+}-free Dulbecco Phosphate-Buffered Saline (DPBS, Euroclone). Cell lysates were obtained according to Ref. 12, resuspended in Sample Buffer (82 mM Tris, 10.5% glycerol, 2% SDS, 0.002% Bromphenol Blue, pH 6.8) supplemented with DTT (100 mM) and urea (125 mg/ml) and incubated for 10 min at 37 °C. Total protein lysates from yeast cells carrying the different PMCA vectors have been prepared according to (16) and finally resuspended in Sample Buffer (0.1 M Tris-Cl pH 8.8; 2% SDS; 50 mM DTT; 10% glycerol; 0.01% Bromphenol Blue).

The total protein content was determined by the Bradford assay (Bio-Rad). Samples were loaded on a 8% SDS-PAGE Tris/HCl gel, transferred onto PVDF membranes (Bio-Rad). The membrane was blocked for 1 h at room temperature using 5% nonfat dried milk (NFDM) in TBST (20 mM Tris-HCl, pH 7.4, 150 mM NaCl, 0.05% Tween-20) and incubated overnight with the specific primary antibody at 4 °C. Monoclonal non isoform specific anti-PMCA clone 5F10, 1:1000 (Thermo Scientific), rabbit polyclonal anti-PMCA3 antibody, 1:1000 (affinity BioReagents) and monoclonal anti-β actin, 1:30000 (Sigma) primary antibodies were used. Detection was carried out by incubation with secondary HRP-conjugated anti-mouse or anti-rabbit IgG antibody (Santa Cruz Biotechnology) for 1.5 h at room temperature. The proteins were visualized by the chemiluminescent reagent Immobilon Western (Millipore).

Immunocytochemistry Analysis—36 h after transfection, HeLa cells were processed for immunofluorescence. The cells were washed twice with PBS (140 mM NaCl 2 mM KCl 1.5 mM KH_2PO_4 8 mM Na_2HPO_4, pH 7.4), fixed for 20 min in 3.7% formaldehyde and washed three times with PBS. The cells were then permeabilized in 0.1% Triton X-100 in PBS, followed by a 1-h wash with 1% gelatin (type IV, from calf skin) in PBS. Cells were then incubated for 1 h at 37 °C in a wet chamber with a monoclonal antibody recognizing all pump isoforms (5F10; Thermo Scientific) or with a rabbit polyclonal anti-PMCA3 antibody (affinity BioReagents) at a 1:100 dilution in PBS. Staining was carried out with Alexa Fluor 488-labeled anti-mouse or anti-rabbit secondary antibody (Molecular Probes, Carlsbad, CA) at a 1:50 dilution in PBS. Fluorescence was analyzed with a Leica SP5 confocal microscope and analyzed by ImageJ software.

Ca^{2+} Measurements with Recombinant Aequorin—Cytosolic Ca^{2+} concentration measurements were carried out in a Perkin-Elmer Envision plate reader equipped with a two-injectors unit. The day before the Ca^{2+} measurements, the transfected cells were plated onto 96-well plate. Recombinant cytAEQ was reconstituted by incubating HeLa cells for 1–3 h with 5 μM coelenterazine in modified Krebs Ringer Buffer (KRB, NaCl 135 mM, KCl 5 mM, KH_2PO_4 400 mM, $MgSO_4$ 1 mM, Hepes 20 mM, pH 7.4). In some experiments the intracellular Ca^{2+} stores were first depleted by incubating the cells for 3 min in KRB containing 1 mM EGTA and supplemented with 1 μM thapsigargin and 100 μM histamine before Ca^{2+} recording. After reconstitution the cells were placed in 70 μl of KRB supplemented as indicated in the figures and luminescence from each well was measured for 1 min. According to the experiment, histamine 100 μM or $CaCl_2$ 3 mM at the final concentration were injected to generate Ca^{2+} transients. The experiments were terminated by lysing the cells with 100 μM digitonin in a hypotonic Ca^{2+}-rich solution (10 mM $CaCl_2$ in H_2O) to discharge the remaining reconstituted aequorin pool. Output data were analyzed and calibrated with a custom made macro-enabled Excel workbook. Data are reported as means ± S.E. Statistical differences were evaluated by Student's two-tailed *t* test for unpaired samples. A *p* value of $\leq$0.05 was considered statistically significant.

Functional Complementation Assay in K616 Yeast Cells—*Saccharomyces cerevisiae* strain K616 (Mat α; *pmr1::HIS3; pmc1::TRP1; cnb1::LEU2; ade2; ura3*) (17) has been used to perform the Ca^{2+}-ATPase functional complementation assays (18). Briefly, yeast cells were transformed by standard protocols (19) with different pYES2-derived vectors, carrying either wild-type or mutagenized PMCA3 cDNAs. Positive clones were selected on SD medium (6.7% yeast nitrogen base with ammonium sulfate, 2% glucose), lacking uracil and added with 10 mM $CaCl_2$. Functional complementation assays (repeated for at least 3–5 independent clones) have been performed by growing yeast cells in SD+$CaCl_2$ until mid-log phase, when similar number of yeast cells were serially diluted and spotted on minimal medium containing glucose (pYES2-PMCA3 repression) or galactose (pYES2-PMCA3 induction) as carbon source. Addition of 10 mM $CaCl_2$ or 10 mM EGTA to glucose or galactose medium reflects permissive and non-permissive conditions for yeast K616 viability, respectively.

Bioinformatics Analysis—SIFT, the polymorphism phenotyping program Poly-Phen and PMut. Computer algorithms were used to analyze the possible impact of *LAMA1* missense mutations. For evolutionary conservation, the LAMA1 and PMCA3 protein sequences were downloaded from NCBI, and the alignments were obtained from Homologene. The prediction of the PMCA3 pump structure has been performed by using Swiss-Model on the SERCA pump structures in its Ca^{2+}-free and Ca^{2+}-bound state (PDB ID:3W5B and 1SU4, respectively) as a template. The obtained structures were analyzed by the Pymol software.

Results

Exome Sequencing Revealed the Presence of Mutations in LAMA1 and ATP2B3 Genes—The proband is a 6-year-old male presenting with global developmental delay, generalized hypotonia and feeding difficulties. His brain MRI at 10 months of age was normal but repeated imaging at 6 years showed unusual vertical course of the straight sinus with inferior location of the torcula, a configuration consistent with a small posterior fossa and a dysplastic corpus callosum (Fig. 1*A*). Whole exome sequencing revealed a maternally inherited hemizygous mutation, p.Arg482His (c.1445G>A), in exon 9 in the X-linked *ATP2B3* gene. This mutation has not been reported previously as a disease-causing mutation nor as a benign polymorphism. The p.Arg482His mutation was not observed in ~6500 individuals of European and African American ancestry in the NHLBI

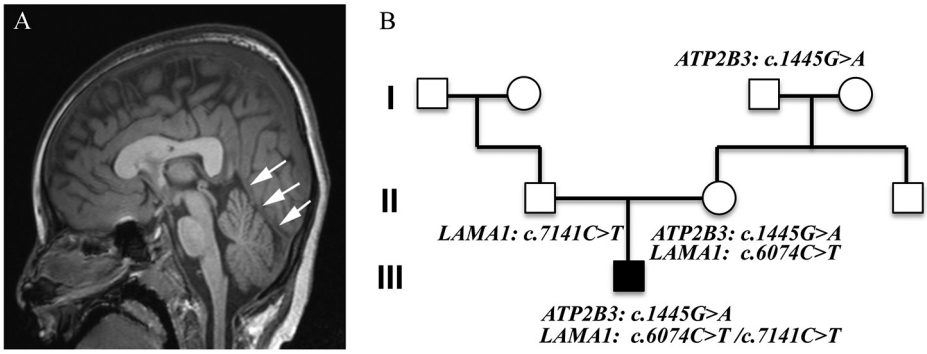

C

	Laminin T2025M	Laminin R2381C		PMCA3 R482H
H.Sapiens	LATSASQSAVS**T**LRDVAGL	VKVMTDLGSGPITLLTDR**R**	H.sapiens	SDKTGTLTTN**R**MTVVQSYLG
P.Troglodytes	LATSASQSAVS**T**LRDVAGL	VKVMTDLGSGPITLLTDR**R**	C.lupus	SDKTGTLTTN**R**MTVVQSYLG
M.Mulatta	LATSASHSAVS**T**LRDVAGL	VKVTTDLGSGPLTLLTDR**R**	B.taurus	SDKTGTLTTN**R**MTVVQSYLG
C.Lupus	LAISVNQSAAN**T**LKNVVGL	VRVVVDLGSGPLALITDR**R**	M.musculus	SDKTGTLTTN**R**MTVVQSYLG
B.Taurus	LAMSANQSATS**T**LKNVMGL	VRVTVDLGSGPLALITDR**R**	R.norvegicus	SDKTGTLTTN**R**MTVVQSYLG
M.Musculus	LAAAANESAVK**T**LEDVLAL	VKVMVDLGSGPLTLMTDR**R**	D.rerio	SDKTGTLTTN**R**MTVVQIYIG
R.Norvegicus	LAVAANETAAR**T**LEDMLGL	VKVMVDLGSGPLTLMTDR**R**	D.melanogaster	SDKTGTLTTN**R**MTVVQSYIC
G.Gallus	LAVSANTSAMV**G**LSHFEDF	VRLTVDLCSGPLALTTEN**R**	A.gambiae	SDKTGTLTTN**R**MTVVQSYIC
D.Rerio	QTEAANASLQE**A**LERLRDY	VHLTFELGSGALTMTSSR**T**	C.elegans	SDKTGTLTTN**R**MTVVQSFVN
X.Tropicalis	LALSANASAAG**T**LSHIMRF	VRVSVELGSGPLVLTSDE**R**	X.tropicalis	SDKTGTLTTN**R**MTVVQSNIG

FIGURE 1. **Phenotype of the proband, pedigree family and multispecies alignment of the LAMA1 and PMCA3 mutations.** *A*, brain imaging of the proband. Single T1-weighted midline sagittal image demonstrates unusual vertical course of the straight sinus (*arrows*) with inferior location of the torcula. This configuration is consistent with a small posterior fossa. *B*, pedigree of the proband's family showing the mapped mutations. *C*, multispecies alignment of the Laminin1 and the PMCA3 amino acids sequences showing that the mutated residues are conserved (*bold*).

Exome Sequencing Project. The maternal grandfather, who reportedly had no neurological findings, is a carrier for the same mutation in the *ATP2B3* gene. In addition, two missense mutations were found in the *LAMA1* gene of the proband: a maternally inherited p.Thr2025Met (c.6074C>T) in exon 43 and a paternally inherited p.Arg2381Cys (c.7141C>T) in exon 50 (Fig. 1*B*) (for the nomenclature of the *LAMA1* gene mutation, nucleotide numbering was designated according to reference sequence in GenBank Accession number NM_005559.3). The p.Thr2025Met mutation was previously reported in one case of somatic mutation in lung carcinoma tumor cells (Cosmic Database ID: COSM708993) but never reported as a disease-causing mutation nor as a benign polymorphism, and not found in ~6500 individuals of European and African American ancestry in the NHLBI Exome Sequencing Project. The p.Arg2381Cys mutation, a rare variant (rs142063208; MAF 0.01), was also reported as somatic mutation in glioblastoma multiforme tumor cells (20). The effect of the p.Thr2025Met was predicted as probably damaging only by the Poly-Phen2 algorithm whereas the p.Arg2381Cys mutation was predicted deleterious by all algorithms used. Alignment of orthologous protein sequences revealed that both Thr-2025 and Arg-2381 residues of laminin subunit 1α and the Arg-428 residue in PMCA3 gene are well conserved across species (Fig. 1*C*).

Comparative Analysis of the Ca^{2+} Handling Activity of the Full Length and Truncated Isoform of WT and R482H PMCA3 Mutant Overexpressed in HeLa Cells—To selectively explore the ability of the mutated PMCA3 pump to handle cellular Ca^{2+} fluxes in living cells, we generated a mammalian expression vector encoding the mutant PMCA3 pump and expressed it in HeLa cells. The R482H mutation was introduced in the full-length (PMCA3b) as well as in a C-terminally truncated (PMCA3a) variant of PMCA3, which is also expressed in neurons, by site-directed mutagenesis. The full-length and the C-terminally truncated isoforms of the pumps only differ in the appearance of a premature stop codon caused by a shift in the reading frame during the alternative splicing of the primary transcript that replaces the C-terminal portion of the pump downstream the middle of the calmodulin-binding domain (4).

Western blotting analysis of the transfected HeLa cells was performed using a non-isoform specific antibody that recognizes all the PMCA variants (5F10) and a rabbit polyclonal anti-PMCA3 antibody. They revealed the presence of pump bands at the expected molecular weight of 135 kDa for the full-length variant and 129 kDa for the truncated variant (Fig. 2, *A* and *B*) with comparable expression levels between the wt and R482H mutant. The numbers under the bands refer to the ratio between the intensities of the bands relative to PMCA and β-actin. The increase over the endogenous level was about 3-fold but, considering that the average transfection efficiency is about 25%, the overexpressed pump should exceed the endogenous one by about 12-fold. We are thus confident that the Ca^{2+} extrusion in PMCA-overexpressing cells is predominantly due to the exogenous pump. The subcellular localization of the overexpressed wt as well as the R482H mutants was assessed by immunocytochemistry analysis. As shown in Fig. 2, *C* and *D*, all the pump variants were correctly targeted to the plasma membrane. Thus, the R482H mutation did not affect the expression or the localization of the transfected pump. Untransfected cells were also visible in Fig. 2*C* (indicated by *arrows*) and the 5F10 antibody revealed that a portion of both the endogenous and the overexpressed PMCA pump was present in the intracellular compartments, possibly in the membrane of the endoplasmic reticulum (ER). We had previously documented that

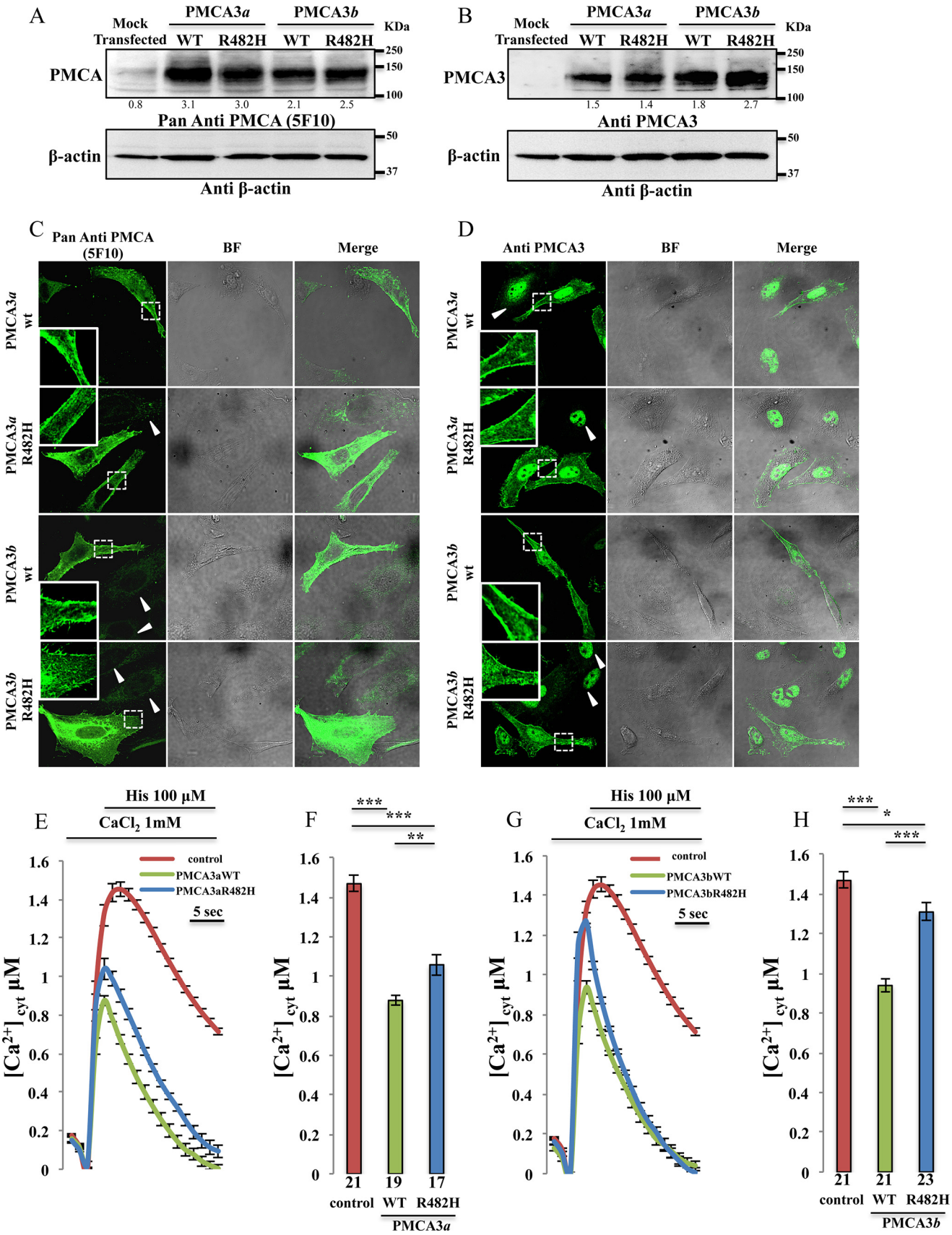

the ER-resident pump was not active, and thus it did not contribute to Ca^{2+} handling (21). The nuclear fluorescence in Fig. 2*D* is a spurious signal, since it is also present in untransfected cells (indicated by *arrows*) where the PMCA3 isoform was absent.

To study whether R482H mutation influenced pump activity we have monitored its ability to counteract the cytosolic Ca^{2+} transients generated upon cell stimulation with an $InsP_3$ generating agonist, which induced Ca^{2+} release from the intracellular stores. HeLa cells were co-transfected with the plasmid encoding the recombinant Ca^{2+}-sensitive photoprotein aequorin (cytAEQ, (14)) and the expression plasmids encoding the mutant PMCA3 isoforms or the respective wt variant. In agreement with previous findings (22), the traces (Fig. 2, *E* and *G*) of the cytosolic Ca^{2+} transients generated by the stimulation with histamine, and their statistical analysis (Fig. 2, *F* and *H*), show that in PMCA3 overexpressing cells the amplitude of the Ca^{2+} peak, regardless of the *a* or *b* splicing variant tested, was significantly reduced with respect to control cells transfected only with cytAEQ (peaks values: 1.46 ± 0.04 μM $n = 21$ for control cells, 0.87 ± 0.02 μM $n = 19$ for wt PMCA3a and, 0.93 ± 0.03 μM $n = 21$ for wt PMCA3b). HeLa cells overexpressing mutant R482H PMCA pumps still displayed Ca^{2+} transients with reduced amplitude and faster kinetics with respect to control cells, indicating that the R482H mutation did not abolish the activity of the pump. However, significant differences in the peak amplitude were observed with respect to the cells overexpressing the wt pump variant (1.05 ± 0.05 μM $n = 17$ for the PMCA3*a* R482H and 1.30 ± 0.04 μM $n = 22$ for the PMCA3*b* R482H), indicating that the activity of the pump was compromised. As a consequence, the cells overexpressing the mutated pump were expected to experience a more prolonged retention of Ca^{2+} within the cytoplasm than those overexpressing the wt pump. This was particularly evident looking at the traces relative to cells overexpressing the *a* variant, *i.e.* the variant which in resting conditions is more active as it is less auto-inhibited (Fig. 2*E*).

Effect of the R482H Mutation on the Ability of PMCA3 to Selectively Control the Ca^{2+} Swings Generated by the Influx of Extracellular Ca^{2+} Promoted by the Emptying of the Intracellular Stores—The Ca^{2+} transients shown in Fig. 2 are the sum of the Ca^{2+} released from the intracellular stores (endoplasmic reticulum and Golgi apparatus) and of the Ca^{2+} influx from the extracellular medium through the store operated Ca^{2+} (SOC) channels. To evaluate the specific contribution of the overexpressed pumps in counteracting Ca^{2+} entry from the extracellular ambient, and to abolish the contribution of Ca^{2+} release from the intracellular deposits and of its re-uptake by the Ca^{2+}-ATPase of the ER (the SERCA pump), the cells were pre-treated for 3 min with a Krebs Ringer Buffer containing the Ca^{2+}-chelating agent EGTA and histamine (to deplete the intracellular stores) in the presence of the inhibitor of the SERCA pump thapsigargin. Cytosolic Ca^{2+} measurements were initiated in a Ca^{2+} free medium, then the cells were exposed to 3 mM extracellular Ca^{2+} to generate cytosolic Ca^{2+} transients through the process of store-operated Ca^{2+} entry (SOCE). Under these conditions, the overexpressed PMCA pumps were forced to work at their maximal rate. Fig. 3 shows the effect of the overexpression of the wt and the R482H mutant pump variants (PMCA3*a* in Fig. 3, *A–C*; PMCA3*b* in Fig. 3, *D–F*). The peak of the transient, which reflected the magnitude of Ca^{2+} influx, was surprisingly significantly higher in cells overexpressing either the wt or the R482H mutated pump than in control cells. This possibly reflected a reduced Ca^{2+}-dependent feedback inhibition of the SOC channels, which in the presence of the overexpressed PMCA pump, and thus under condition of local increased Ca^{2+} extrusion, were exposed to sub-plasma membrane microdomains of reduced Ca^{2+} concentrations or duration (peak values in μM ± S.E. were: 6.24 ± 0.32 $n = 20$ for control cells, 8.54 ± 0.38 $n = 22$ for the wt PMCA3a, 9.31 ± 0.52 $n = 20$ for R482H PMCA3a and 9.36 ± 0.51 $n = 20$ for wt PMCA3b, 9.89 ± 0.67 $n = 20$ for the R482H PMCA3b). As the Ca^{2+} peaks declined, the traces attained a plateau level (enlarged *insets* in Fig. 3, *A* and *D*), which reflected the average amount of cytosolic Ca^{2+} concentration in the post-influx phase, and permitted a better assessment of the pump extrusion ability. The cells overexpressing the wt and mutated PMCA3 variants attained a lower basal Ca^{2+} plateau than control cells, as they expressed increased pump amount. As for the comparison between wt *versus* mutated PMCA3 pumps, the average basal Ca^{2+} concentration values were slightly, but significantly, higher in cells overexpressing the R482H PMCA mutant pumps than in those overexpressing the wt variants (Fig. 3*C* for the PMCA3*a* variant. The plateau values in μM ± S.E. were: 0.56 ± 0.01 $n = 20$ for the wt and 0.64 ± 0.03 $n = 22$ for the R482H mutant; Fig. 3*F* for the PMCA3*b* variant, plateau values in μM ± S.E. were: 0.62 ± 0.02 $n = 18$ for wt and 0.72 ± 0.03 $n = 22$ for the R482H mutant PMCA3,$p < 0.00001$). The results thus confirmed that the introduction of R482H mutation in both *a* and *b* pump variants impaired their efficiency in maintaining basal Ca^{2+} levels, causing sustained Ca^{2+} retention in the cytoplasm.

Effect of the R482H Mutation on the Basal Activity of PMCA3 Assessed by Functional Complementation Assay in K616 Yeast Cells—To better evaluate the effect of the R482H mutation on pump basal activity, *i.e.* on the activity of the auto-inhibited state of the pump only exposed to the nM concentration of Ca^{2+} that prevails in the cytoplasm at rest, a yeast-based functional assay, which has been previously described, was employed (23). In this assay, the lethal phenotype of the K616 triple mutant

FIGURE 2. **Analysis of the expression of the exogenous pump variants and cytosolic Ca^{2+} measurements in HeLa cells overexpressing the wt and the mutant PMCA3 isoforms.** *A* and *B*, Western blotting. *C* and *D*, immunocytochemistry analysis showing the expression level and the intracellular distribution of the PMCA3 pump in HeLa cells expressing the wt and the mutant truncated (*a*) as well as full-length (*b*) variants. The PMCA3 was revealed by the mouse monoclonal antibody 5F10 in *A* and *C*, and by the rabbit polyclonal anti-PMCA3 antibody in *B* and *D*. *E–H*, cells were co-transfected with cytAEQ and the expression plasmid for the a (*E-F*) or the b (*G-H*) wt as well as the mutated PMCA3 variants. Cytosolic Ca^{2+} transients (*E–G*) were recorded following 100 μM histamine stimulation. The average peak values are shown in (*F-H*). Bars in *panels F* and *H* represent mean [Ca^{2+}] values upon stimulation (μM ± S.E.). ***, $p < 0.001$; **, $p < 0.01$; *, $p \leq 0.05$. The number on the bars indicate the number of independent measurements out of six independent transfections.

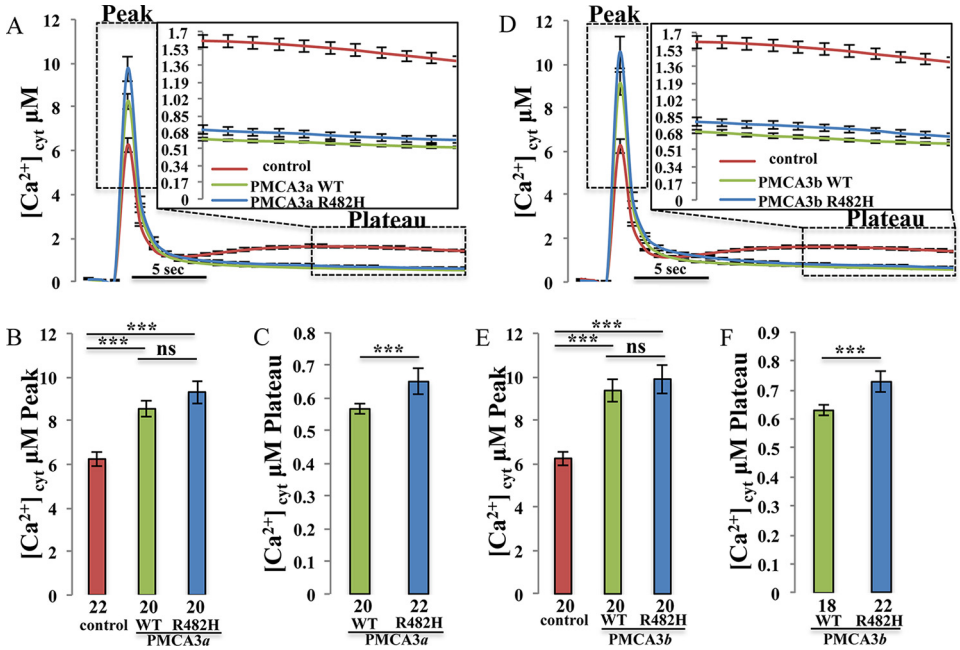

FIGURE 3. **Effect of the truncated and full length wt and mutant pump on the influx of Ca^{2+} from the extracellular medium.** HeLa cells were co-transfected with cytAEQ and the PMCA3 constructs, or transfected with cytAEQ only, pretreated with 1 μM thapsigargin and 100 μM histamine in a buffer containing 1 mM EGTA for 3 min and perfused in the presence of KRB/Ca^{2+} 3 mM to stimulate Ca^{2+} entry from the extracellular ambient. The Ca^{2+} transients in *panel A* for the PMCA3a isoform and in *panel D* for the b variant are characterized by a first peak and a plateau phase (as indicated). Enlargements of the plateau phases are shown in the *insets*. *Panels B* and *E* show the averaged peak [Ca^{2+}] values obtained upon stimulation and *panels C* and *F* show the obtained averaged [Ca^{2+}] values of the plateau. Bars represent means ± S.E. obtained by averaging the values obtained in at least 18 independent measurements from six independent transfections for each condition. ***, $p < 0.001$; *ns*, not significant.

yeast cells observed in Ca^{2+}-free conditions can be rescued by the ectopic expression of active Ca^{2+} pumps. To test the system, two control PMCA3 mutants were generated: an ATPase-dead mutant in which the catalytic aspartate residue of the pump was replaced with an alanine (PMCA3*b* D465A), and a C-terminally truncated PMCA3 mutant lacking nearly the entire autoinhibitory C-terminal tail (the last 158 C-terminal residues, PMCA3-ΔC_{ter}). The removal of the C-terminal tail renders the pump constitutively active, making this variant a suitable positive control in the assay.

Yeast K616 cells were transformed with the galactose-inducible plasmid pYES encoding the wt pump, or with the PMCA3*b* D465A, the PMCA3-ΔC_{ter}, and the PMCA3*b* R482H pump variants. Fig. 4*A* shows the growth controls of yeast transformed with the different PMCA3 constructs in a Ca^{2+}-containing permissive medium (glucose + $CaCl_2$) or in an inducible Ca^{2+}-free medium (galactose + EGTA), and Fig. 4*B* shows the Western blotting analysis of the PMCA3 pump protein expression levels.

As expected, the PMCA3*b*-ΔC_{ter} mutant that lacked the C-terminal tail, and was thus constitutively active, was able to fully rescue the viability of K616 yeast cells in the Ca^{2+}-depleted medium, whereas the wt PMCA3b, which was auto-inhibited, did it only partially (Fig. 4*A*). Again as expected, the ATPase-dead PMCA3*b* D465A mutant failed to rescue the viability of the K616 yeast cells (Fig. 4*A*). Fig. 4*C* shows the effect of the PMCA3*b* R482H mutant in comparison with the wt and the constitutively active PMCA3*b*-ΔC_{ter} variant. The R482H mutant was clearly defective in the recovery of the viability of the K616 cells. The mutant pump did still permit some recovery of yeast viability, *i.e.* it evidently did not completely turn off the basal, unstimulated activity of the pump. This was in agreement with the results of the experiments on the overexpression of the mutated pump in HeLa cells that had shown that the R482H PMCA3 mutant, even if defective, was still active. The Western blot analysis of the total protein extracts from yeast cells grown in the galactose medium show that all PMCA3 constructs were expressed in yeast cells at comparable levels (Fig. 4, *B* and *D* for the different PMCA3*b* variants). The experiments in Fig. 4 thus shows that the defect induced by the R482H mutation also affected the basal unstimulated activity of the pump.

In Silico Analysis of the Effects of the R482H Mutation on PMCA3 Pump Structure—In an attempt to understand the consequences of the R482H mutation on the structure of the pump, we decided to perform an *in silico* modeling study using the SERCA pump 3D structure in the Ca^{2+}-free and Ca^{2+}-bound states (PDB ID:3W5B) and (PDB ID: 1SU4) (Fig. 5, *A* and *D*, respectively). The 3D structure defines the membrane sector of the pump containing 10 helices, and the three large cytosolic domains: the ATP binding N domain protruding into the cytosol between trans-membrane domains 4 and 5, the P domain that contains the catalytic Asp (blue dots), and the A domain (the actuator domain) that performs the de-phosphorylation of the catalytic Asp-P. During the reaction cycle, a series of conformational transformations have been shown to occur in both the cytosolic and the membrane sectors of the SERCA pump, the most evident being the transition of the cytosolic portion from a compact arrangement in the Ca^{2+}-free state (Fig. 5*A*) to a looser state in its presence (Fig. 5*D*). A finer analysis of the structure of the modeled PMCA3 pump identifies glutamate 530 as critical for short-range interactions with the Arg-482

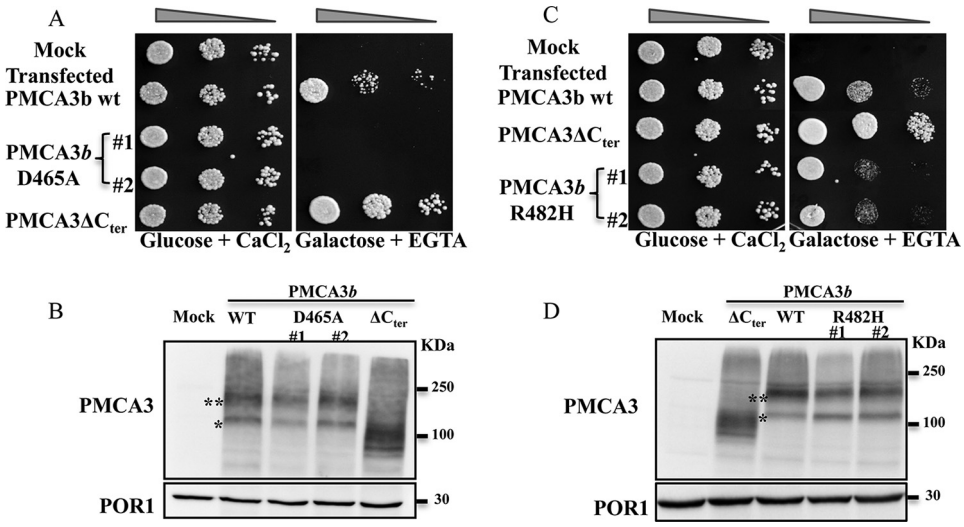

FIGURE 4. **Functional complementation assay in K616 yeast cells.** *A*, serial dilutions and *B* Western blotting analysis of yeast K616 cells transformed with pYES2-derived vectors carrying wild-type, D465A mutant, or the C-terminal truncated PMCA3 (PMCAΔ3C$_{ter}$). Empty vector pYES2 (mock transfected) was used as negative control. *C* and *D*, same as *A-B* but yeast K616 cells are transformed with pYES2-derived vectors carrying wild-type, R482H mutant, or the PMCAΔ3C$_{ter}$. Total protein lysates from yeast cells carrying the indicated pYES2-derived plasmids were probed with anti-PMCA antibody 5F10. Both monomeric (*) and dimeric (**) PMCA3 forms were detected.

residue. In the wt PMCA3 pump in the Ca^{2+}-free state, Arg-482 is at a distance of 9.2 Å from Glu-530 (Fig. 5*B*), the distance increasing to 11.6 Å if the position 482 is occupied by a histidine (Fig. 5*C*). These distances obviously do not permit the interaction between the two residues. However, in the Ca^{2+}-bound state (Fig. 5, *E* and *F*), the guanidinium nitrogens of Arg-482 are now at a distance from both carboxylic oxygens of Glu-530 that permits interaction: 2.66 Å for each of them (Fig. 5*E*). The interaction could be critical for the stabilization of this portion of the PMCA3 pump in the Ca^{2+}-bound state. However, when position 482 becomes occupied by a histidine (Fig. 5*F*), its nitrogen lies at a distance of 4.5 Å and 4.3 Å from the oxygens of Glu-530, respectively. These increased distances could well reduce the stabilization of this portion of the pump in the Ca^{2+}-bound state. The intrinsic pH-dependence of histidine might also have a role in the modulation of the stability of this portion of the pump molecule.

Discussion

Genetic defects of calcium pumps (the Golgi (SPCA) pump, the sarco(endo)plasmic reticulum (SERCA) pump, and the plasma membrane (PMCA) pump) are the cause of a number of diseases. The hereditary deafness caused by mutations of the PMCA2 isoform (7, 9) can be associated with ataxic symptoms (10, 11). An ataxia-causing defect was recently described in PMCA3 (12). The present contribution describes a second case of ataxia in which the proband carries a defect in the PMCA3 pump. The defect was evident in both the maximally activated Ca^{2+} exporting function of the pump and in its resting activity, in which the pump was expected to be largely auto-inhibited. The overall malfunction of the enzyme in both the fully active and in the resting states was not surprising, as the mutation concerned a residue close to its active center. The *in silico* analysis shown in Fig. 5 has offered a plausible molecular rationale for the inhibitory effect of the mutation.

The finding of a second ataxic proband who carries an *ATP2B3* mutation suggests that defects of the PMCA3 pump could perhaps be specifically associated to the ataxic pathology. A peculiar property of PMCA pumps is the phenomenon of auto-inhibition in the resting, low Ca^{2+} state. It is produced by the binding of the C-terminal tail of the pump to its main body, and is relieved by the binding of calmodulin once Ca^{2+} in the ambient increases. Thus, mutations could positively or negatively affect the auto-inhibition process and/or inhibit the Ca^{2+} exporting function of the pump in the fully active state (24, 25). It should also be mentioned that the Ca^{2+} exporting function of the pump in cells in which the much more powerful Na^+/Ca^{2+} exchanger predominates, *e.g.* in muscles and neurons, is of marginal importance to the global regulation of cell Ca^{2+} (26), but is very important to the regulation of Ca^{2+} in the microdomains surrounding the cytosolic portion of the pump. The PMCA pump has been shown to be concentrated in the caveolae, which also contain enzyme supercomplexes that are essential for cell functions (27, 28). Neurons do not contain caveolae, but contain functionally equivalent structural microdomains, *e.g.* the spines. Pump defects could thus have important consequences for the local regulation of intracellular Ca^{2+} signaling with very serious deleterious effects on the activity of the cell. One last important point should be mentioned, as it may be significant to the role of PMCA pump defects in pathology. As it has become clear from the studies of hereditary hearing loss, the mutation in the *ATP2B2* gene acted synergistically with a defect of *CDH23* or *MYO6* to induce the pathological phenotype by a digenic disease-causing mechanism. In the proband described here, the defect of the PMCA3 pump is not isolated, as he also carries compound heterozygous mutations in *LAMA1*. Interestingly, his maternal grandfather carries the PMCA3 mutation and is apparently healthy, which raises questions regarding incomplete penetrance secondary to genetic modifiers. We suggest that the PMCA3 mutation, may contribute or enhance ataxic symptoms in the presence of the two *LAMA1* mutations in our proband. Laminins are extracellular matrix proteins essential for basement membranes assembly

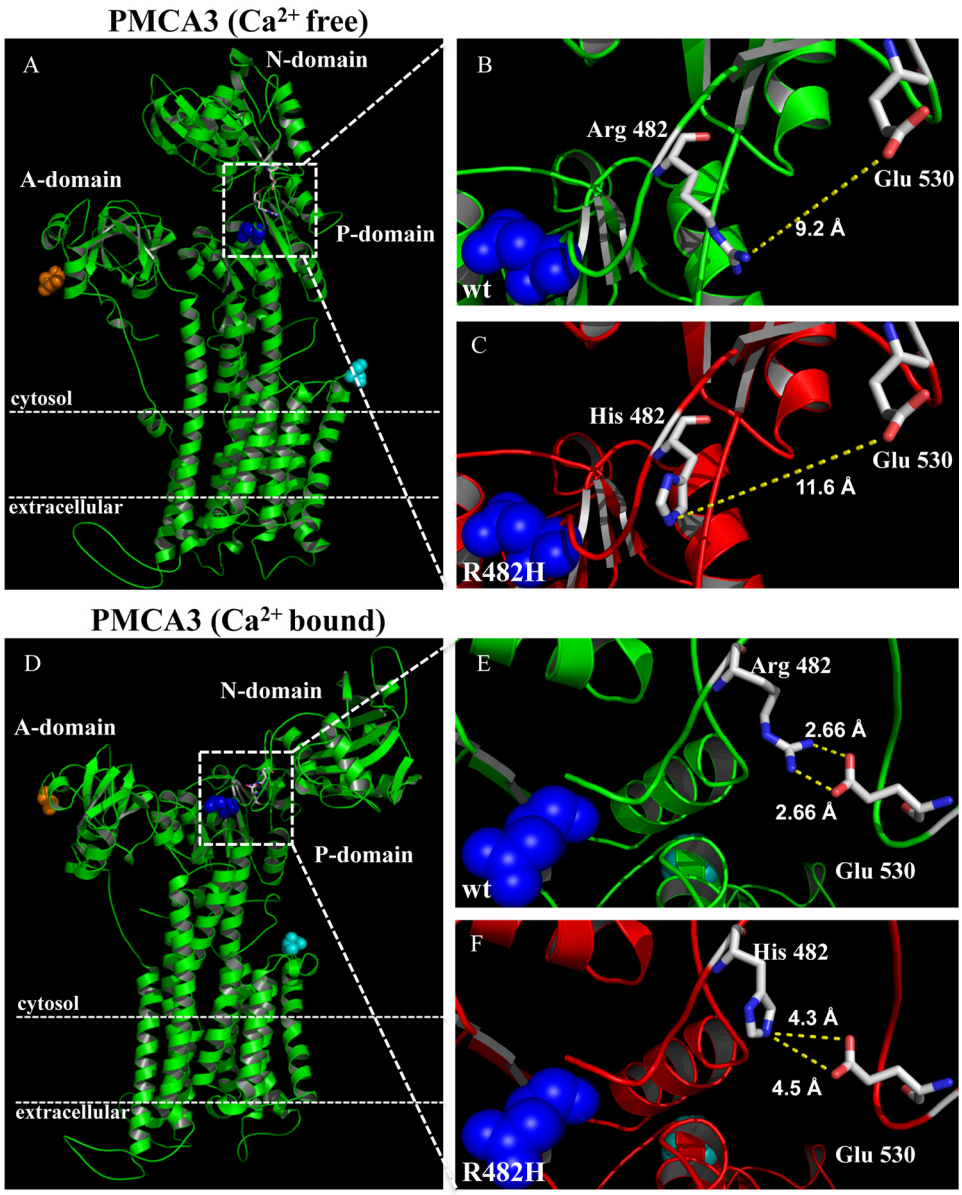

FIGURE 5. **Structural changes induced by the R482H mutation in the PMCA3 pump.** *A*, Ca^{2+}-free and *D*, Ca^{2+}-bound structures of the wt (*B* and *E*) and R482H-mutated (*C* and *F*) PMCA3 pumps were built on the basis of the respective SERCA structures (PDB 3W5B and 1SU4, respectively). The *blue dots* represent the catalytic aspartate and the Arg-482 and the His-482 residues are shown as stick together with the Glu-530 residue. The N terminus and the C terminus of the pump are shown as *orange* and *cyan dots*, respectively.

(29), and *LAMA1* is essential for mouse cerebellar development: its deficiency causes a decrease in the proliferation and migration of granule cells precursors and a marked reduction of dendritic processes in Purkinje cells (30). Mutations in *PMCA3* and *LAMA1* could thus work synergistically, and contribute to the disease phenotype of our proband. This is still a speculative suggestion since it cannot be excluded that the two *LAMA1* mutations would be sufficient *per se* to cause the phenotype. The malfunction of the systems that control Ca^{2+} could naturally be expected to have negative consequences for neurons, given the special importance of Ca^{2+} signaling to them. However, the synergism between a defect of *LAMA1* and that of a Ca^{2+}-related protein is not as immediately obvious as that of the PMCA2 pump with Ca^{2+}-related Cadherin-23 in hereditary deafness. It might be interesting that another laminin, β-2 laminin, has recently been shown to be involved in the process of maturation and Ca^{2+} sensitivity of voltage-gated Ca^{2+} channels (31).

Acknowledgments—Ethics Statement: The parents of the proband signed a Media Authorization for the Use and Disclosure Protected Health Information form approved by The Washington University School of Medicine Institutional Review Board. The authors declare that they have no conflicts of interest with the contents of this article.

References

1. Brini, M., Calì, T., Ottolini, D., and Carafoli, E. (2013) Intracellular calcium homeostasis and signaling. *Metal Ions in Life Sciences* **12,** 119–168
2. Carafoli, E. (2007) The unusual history and unique properties of the calcium signal in *New Comprehensive Biochemistry* (Joachim, K., and Marek,

M., eds), pp. 3–22, Elsevier
3. Brini, M., Calì, T., Ottolini, D., and Carafoli, E. (2014) Neuronal calcium signaling: function and dysfunction. *Cell Mol. Life Sci.* **15,** 2787–2814
4. Brini, M., and Carafoli, E. (2009) Calcium pumps in health and disease. *Physiol. Rev.* **89,** 1341–1378
5. Eakin, T. J., Antonelli, M. C., Malchiodi, E. L., Baskin, D. G., and Stahl, W. L. (1995) Localization of the plasma membrane Ca(2+)-ATPase isoform PMCA3 in rat cerebellum, choroid plexus and hippocampus. *Brain Res. Mol. Brain Res.* **29,** 71–80
6. Dumont, R. A., Lins, U., Filoteo, A. G., Penniston, J. T., Kachar, B., and Gillespie, P. G. (2001) Plasma membrane Ca2+-ATPase isoform 2a is the PMCA of hair bundles. *J. Neurosci.* **21,** 5066–5078
7. Ficarella, R., Di Leva, F., Bortolozzi, M., Ortolano, S., Donaudy, F., Petrillo, M., Melchionda, S., Lelli, A., Domi, T., Fedrizzi, L., Lim, D., Shull, G. E., Gasparini, P., Brini, M., Mammano, F., and Carafoli, E. (2007) A functional study of plasma-membrane calcium-pump isoform 2 mutants causing digenic deafness. *Proc. Natl. Acad. Sci. U.S.A.* **104,** 1516–1521
8. Bortolozzi, M., Brini, M., Parkinson, N., Crispino, G., Scimemi, P., De Siati, R. D., Di Leva, F., Parker, A., Ortolano, S., Arslan, E., Brown, S. D., Carafoli, E., and Mammano, F. (2010) The novel PMCA2 pump mutation Tommy impairs cytosolic calcium clearance in hair cells and links to deafness in mice. *J. Biol. Chem.* **285,** 37693–37703
9. Schultz, J. M., Yang, Y., Caride, A. J., Filoteo, A. G., Penheiter, A. R., Lagziel, A., Morell, R. J., Mohiddin, S. A., Fananapazir, L., Madeo, A. C., Penniston, J. T., and Griffith, A. J. (2005) Modification of human hearing loss by plasma-membrane calcium pump PMCA2. *N. Engl. J. Med.* **352,** 1557–1564
10. Inoue, Y., Matsumura, Y., Inoue, K., Ichikawa, R., and Takayama, C. (1993) Abnormal synaptic architecture in the cerebellar cortex of a new dystonic mutant mouse, Wriggle Mouse Sagami. *Neurosci. Res.* **16,** 39–48
11. Empson, R. M., Turner, P. R., Nagaraja, R. Y., Beesley, P. W., and Knöpfel, T. (2010) Reduced expression of the Ca(2+) transporter protein PMCA2 slows Ca(2+) dynamics in mouse cerebellar Purkinje neurones and alters the precision of motor coordination. *J. Physiol.* **588,** 907–922
12. Zanni, G., Calì, T., Kalscheuer, V. M., Ottolini, D., Barresi, S., Lebrun, N., Montecchi-Palazzi, L., Hu, H., Chelly, J., Bertini, E., Brini, M., and Carafoli, E. (2012) Mutation of plasma membrane Ca2+ ATPase isoform 3 in a family with X-linked congenital cerebellar ataxia impairs Ca2+ homeostasis. *Proc. Natl. Acad. Sci. U.S.A.* **109,** 14514–14519
13. Aldinger, K. A., Mosca, S. J., Tétreault, M., Dempsey, J. C., Ishak, G. E., Hartley, T., Phelps, I. G., Lamont, R. E., O'Day, D. R., Basel, D., Gripp, K. W., Baker, L., Stephan, M. J., Bernier, F. P., Boycott, K. M., Majewski, J., University of Washington Center for Mendelian, G., Care4Rare, C., Parboosingh, J. S., Innes, A. M., and Doherty, D. (2014) Mutations in LAMA1 cause cerebellar dysplasia and cysts with and without retinal dystrophy. *Am. J. Hum. Genet.* **95,** 227–234
14. Brini, M., Marsault, R., Bastianutto, C., Alvarez, J., Pozzan, T., and Rizzuto, R. (1995) Transfected aequorin in the measurement of cytosolic Ca2+ concentration ([Ca2+]c). A critical evaluation. *J. Biol. Chem.* **270,** 9896–9903
15. Rizzuto, R., Brini, M., Bastianutto, C., Marsault, R., and Pozzan, T. (1995) Photoprotein-mediated measurement of calcium ion concentration in mitochondria of living cells. *Methods Enzymol.* **260,** 417–428
16. Cox, J. S., Chapman, R. E., and Walter, P. (1997) The unfolded protein response coordinates the production of endoplasmic reticulum protein and endoplasmic reticulum membrane. *Mol. Biol. Cell* **8,** 1805–1814
17. Cunningham, K. W., and Fink, G. R. (1994) Calcineurin-dependent growth control in *Saccharomyces cerevisiae* mutants lacking PMC1, a homolog of plasma membrane Ca2+ ATPases. *J. Cell Biol.* **124,** 351–363
18. Baekgaard, L., Luoni, L., De Michelis, M. I., and Palmgren, M. G. (2006) The plant plasma membrane Ca2+ pump ACA8 contains overlapping as well as physically separated autoinhibitory and calmodulin-binding domains. *J. Biol. Chem.* **281,** 1058–1065
19. Gietz, R. D., and Woods, R. A. (2002) Transformation of yeast by lithium acetate/single-stranded carrier DNA/polyethylene glycol method. *Methods Enzymol.* **350,** 87–96
20. Mao, P., Joshi, K., Li, J., Kim, S. H., Li, P., Santana-Santos, L., Luthra, S., Chandran, U. R., Benos, P. V., Smith, L., Wang, M., Hu, B., Cheng, S. Y., Sobol, R. W., and Nakano, I. (2013) Mesenchymal glioma stem cells are maintained by activated glycolytic metabolism involving aldehyde dehydrogenase 1A3. *Proc. Natl. Acad. Sci. U.S.A.* **110,** 8644–8649
21. Brini, M., Bano, D., Manni, S., Rizzuto, R., and Carafoli, E. (2000) Effects of PMCA and SERCA pump overexpression on the kinetics of cell Ca(2+) signalling. *EMBO J.* **19,** 4926–4935
22. Brini, M., Coletto, L., Pierobon, N., Kraev, N., Guerini, D., and Carafoli, E. (2003) A comparative functional analysis of plasma membrane Ca2+ pump isoforms in intact cells. *J. Biol. Chem.* **278,** 24500–24508
23. Ton, V. K., and Rao, R. (2004) Functional expression of heterologous proteins in yeast: insights into Ca2+ signaling and Ca^{2+}-transporting ATPases. *Am. J. Physiol. Cell Physiol* **287,** C580-C589
24. Enyedi, A., Vorherr, T., James, P., McCormick, D. J., Filoteo, A. G., Carafoli, E., and Penniston, J. T. (1989) The calmodulin binding domain of the plasma membrane Ca2+ pump interacts both with calmodulin and with another part of the pump. *J. Biol. Chem.* **264,** 12313–12321
25. Verma, A. K., Enyedi, A., Filoteo, A. G., and Penniston, J. T. (1994) Regulatory region of plasma membrane Ca2+ pump. 28 residues suffice to bind calmodulin but more are needed for full auto-inhibition of the activity. *J. Biol. Chem.* **269,** 1687–1691
26. Lopreiato, R., Giacomello, M., and Carafoli, E. (2014) The plasma membrane calcium pump: new ways to look at an old enzyme. *J. Biol. Chem.* **289,** 10261–10268
27. Fujimoto, T. (1993) Calcium pump of the plasma membrane is localized in caveolae. *J. Cell Biol.* **120,** 1147–1157
28. Hammes, A., Oberdorf-Maass, S., Rother, T., Nething, K., Gollnick, F., Linz, K. W., Meyer, R., Hu, K., Han, H., Gaudron, P., Ertl, G., Hoffmann, S., Ganten, U., Vetter, R., Schuh, K., Benkwitz, C., Zimmer, H. G., and Neyses, L. (1998) Overexpression of the sarcolemmal calcium pump in the myocardium of transgenic rats. *Circulation Research* **83,** 877–888
29. Powell, S. K., and Kleinman, H. K. (1997) Neuronal laminins and their cellular receptors. *Int. J. Biochem. Cell Biol.* **29,** 401–414
30. Heng, C., Lefebvre, O., Klein, A., Edwards, M. M., Simon-Assmann, P., Orend, G., and Bagnard, D. (2011) Functional role of laminin α1 chain during cerebellum development. *Cell Adhesion and Migration* **5,** 480–489
31. Chand, K. K., Lee, K. M., Schenning, M. P., Lavidis, N. A., and Noakes, P. G. (2014) Loss of beta2-laminin alters calcium sensitivity and voltage-gated calcium channel maturation of neurotransmission at the neuromuscular junction. *J Physiol.* **593,** 245–265

A Novel Mutation in Isoform 3 of the Plasma Membrane Ca^{2+} Pump Impairs Cellular Ca^{2+} Homeostasis in a Patient with Cerebellar Ataxia and Laminin Subunit 1 α Mutations

Tito Calì, Raffaele Lopreiato, Joshua Shimony, Marisa Vineyard, Martina Frizzarin, Ginevra Zanni, Giuseppe Zanotti, Marisa Brini, Marwan Shinawi and Ernesto Carafoli

J. Biol. Chem. 2015, 290:16132-16141.
doi: 10.1074/jbc.M115.656496 originally published online May 7, 2015